Sequential proteolysis and high-field FTICR MS to determine disulfide connectivity and 4-maleimide TEMPO spin-label location in L126C GM2 activator protein

6 AUTHORS, INCLUDING:

Jeremiah D Tipton

SCIEX

21 PUBLICATIONS **573** CITATIONS

SEE PROFILE

Gail E Fanucci

University of Florida

87 PUBLICATIONS **1,407** CITATIONS

SEE PROFILE

Sequential Proteolysis and High-Field FT-ICR MS to Determine Disulfide Connectivity and 4-Maleimide TEMPO Spin-Label Location in L126C GM2 Activator Protein[1]

Jeremiah D. Tipton[‡], **Jeffrey D. Carter**[§], **Jordan D. Mathias**[§], **Mark R. Emmett**[†,‡], **Gail E. Fanucci**[§,*], and **Alan G. Marshall**[†,‡,*]

[†]Ion Cyclotron Resonance Program, National High Magnetic Field Laboratory, Florida State University, 1800 East Paul Dirac Drive, Tallahassee, FL 32310-4005

[§]Department of Chemistry, University of Florida, PO Box 117200, Gainesville, Florida 32611

[‡]Department of Chemistry and Biochemistry, 95 Chieftain Way, Florida State University, Tallahassee, FL 32306-4390

Abstract

The GM2 activator protein (GM2AP) is an 18 kDa non-enzymatic accessory protein involved in the degradation of neuronal gangliosides. Genetic mutations of GM2AP can disrupt ganglioside catabolism and lead to deadly lysosomal storage disorders. Crystallography of wild-type GM2AP reveals 4 disulfide bonds and multiple conformations of a flexible loop region that is thought to be involved in lipid binding. To extend the crystallography results, a cysteine construct (L126C) was expressed and modified with 4-maleimide TEMPO for electron paramagnetic resonance (EPR) studies. However, because a ninth cysteine has been added by site-directed mutagenesis and the protein was expressed in *E. coli* in the form of inclusion bodies, the protein could misfold during expression. To verify correct protein folding and labeling, a sequential multiple-protease digestion, nano-LC electrospray ionization 14.5 T Fourier transform ion cyclotron resonance mass spectrometry assay was developed. High-magnetic field and robust automatic gain control results in sub-ppm mass accuracy for location of the spin-labeled cysteine and verification of proper connectivity of the four disulfide bonds. The sequential multiple protease digestion strategy and ultra-high mass accuracy provided by FT-ICR MS allow for rapid and unequivocal assignment of relevant peptides and provide a simple pipeline for analyzing other GM2AP constructs.

INTRODUCTION

The GM2 Activator Protein (GM2AP) is an 18 kDa, non-enzymatic accessory protein involved in ganglioside catabolism. A specific function of GM2AP involves binding and extracting GM2 from intralysosomal vesicles that positions the terminal GalNAc head group of GM2 for cleavage by β-hexosaminidase A (Hex A) to produce GM3.[1, 2] Genetic mutations to either GM2AP or Hex A prevent the degradation of GM2, thereby causing lysosomal storage disease, such as AB variant gangliosidosis and Tay Sachs disease.[3–5] GM2AP X-ray crystallographic structures reveal 4 disulfide bonds and a β-cup topology that forms a hydrophobic pocket for

lipid binding.[6] Various X-ray structures with different lipid substrates reveal multiple conformations of a mobile loop region that is observed in either a "closed" or "open" conformation. These "open" and "closed" conformations suggest a functional conformation change that may occur upon lipid ligand or vesicle binding.[6]

To further probe the "binding" conformational changes of the loop region, site-directed spin labeling electron paramagnetic resonance (EPR) spectroscopy[7–10] was applied to GM2AP.[11] In proteins, site-directed spin labeling typically proceeds by generating site-specific cysteine amino acid substitutions for modification with paramagnetic nitroxide probes, e.g., 4-maleimide-TEMPO (Figure 1). Reduced cysteine residues act as nucleophiles capable of reacting with maleimide or thiosulfonate groups to form thioethers or disulfide bonds, respectively. Cysteine residues involved in disulfide bonds do not readily react with those functional groups at pH 6.8–7.4.[12] To ensure that purified protein contained the proper connectivity of the 8 native cysteine residues and that only the introduced reporter cysteine (L126C) was labeled, a mass spectrometry based assay was developed.

Mass spectrometry enables direct identification of post-translational modifications, including disulfide bonds.[13–20] Because of the analytical challenge associated with verifying multiple disulfide bonds, a multi-tier assay was developed. First, the expressed protein was sequentially proteolytically digested with the enzymes, trypsin, endoproteinase GluC, and endoproteinase AspN. After each sequential digestion, the samples were analyzed by high-field Fourier transform ion cyclotron resonance (FT-ICR) MS.[21] Although sequential proteolysis produces more complex mixtures for analysis, the resulting MS/MS spectra from *less complex* disulfide-bound peptide fragments result in simple *verification* of disulfide connectivity. High resolution mass measurement with our modified 14.5 T LTQ FT-ICR MS provides high mass accuracy and allows for quick peptide and fragment ion assignments with rms mass errors of less than 0.5 ppm.[21] Here, we present a systematic approach to verify proper folding and labeling of a recombinantly over-expressed L126C GM2AP construct by combination of standard proteomic techniques and multiple scan functions with high resolution MS and/or low/high resolution MS/MS with our modified 14.5 T LTQ FT-ICR MS. The first scan function included the use of the typical top-5 data dependent (high resolution MS; low resolution MS/MS) to *identify* all proteolytic fragments, whereas the identified fragments were subsequently analyzed by directed high resolution MS/MS for *verification* of disulfide connectivity. Furthermore, electron capture dissociation (ECD) with our custom-built 9.4 T FT-ICR provided the last piece of information for verification of disulfide binding. The result is a high-confidence MS assay that will be easy to apply to other spin-labeled proteins containing multiple disulfide linkages.

EXPERIMENTAL PROCEDURES

Materials

All solvents, methanol and water, were purchased from J.T. Baker (Philipsburg, NJ) at HPLC grade. Trypsin, endoproteinase GluC, endoproteinase Asp N, formic acid, and ammonium bicarbonate were purchased from Sigma-Aldrich (St. Louis, MO).

Protein Expression and Purification of GM2AP Mutants

Wild-type and L126C GM2AP constructs were purified as previously described.[22] The substituted cysteine residue was modified with 4-maleimide-TEMPO (4MT) overnight in the dark (4 °C) in 25 mM Tris, 2.5% glycerol, and 0.05% Tween 20 buffer (pH 7.0). The spin-labeled L126C-4MT GM2AP construct was then dialyzed against 25 mM Tris, 2.5% glycerol, and 0.05% Tween 20 buffer (pH 8.0) and concentrated to 200 μL. Concentrated spin-labeled protein was loaded onto a size-exclusion S-200 Sephacryl column (Amhersham Biosciences,

Piscataway, NJ) and eluted with 25 mM ammonium bicarbonate (pH 8.0) to remove the salts and detergents.

Sequential Digestion with Trypsin, GluC, and AspN

The solvent-exchanged sample was diluted to 50 pmol/µL (i.e., 50 µM), with a final volume of 160 µL. To that solution, 100 ng of trypsin (final substrate:trypsin ratio ~1000:1) was added and incubated overnight at 36 °C. Next, a 100 µL aliquot of the trypsin digest was incubated overnight with 200 ng of endoproteinase GluC (substrate:GluC, 400:1) at 36 °C. Finally, 50 µL of the trypsin/Glu C digested solution was incubated with 100 ng of endoproteinase AspN (substrate:AspN, 400:1). Each sample was diluted to 1 pmol/µL prior to LC MS analysis.

Direct Infusion and Reversed-Phase Capillary Liquid Chromatography

Direct infusion of the intact proteins was performed with an Advion BioSystems Nanomate (Ithaca, NY).[23] The intact proteins were diluted to 1–5 pmol/µL in H_2O/methanol/formic acid, 43/50/2 (v/v/v). Digests were separated by reversed-phase nano-liquid chromatography (10 µL sample) with a C_{18} capillary column (New Objective, Woburn, MA] 5 cm× 75 µm, 15 µm i.d spray tip). An Eksigent NanoLC (Dublin, CA) was used to deliver a 35 minute gradient (5 to 95% B) at 400 nL/min with solution A as 0.5% formic acid (v/v) in 5% aqueous methanol and solution B as 0.5% formic acid (v/v) in 95% aqueous methanol.

Mass Spectrometry

Mass spectrometry was performed with either a modified hybrid linear quadrupole ion trap FT-ICR mass spectrometer (LTQ-FT, Thermo Fisher Corp., Bremen, Germany) equipped with an actively shielded 14.5 T superconducting magnet (Magnex, Oxford, U.K.),[21, 24, 25] or a custom-built 9.4 T FT-ICR MS.[26–28] The protease-treated samples were screened by on-line LC/MS with the 14.5 T LTQ FT-ICR instrument operated in top-5 data-dependent mode (high resolution FT-ICR, low resolution LTQ CID MS/MS. For each precursor ion measurement, one million charges were accumulated in the LTQ prior to transfer (~1 ms transfer period) through three octopole ions guides (2.2 MHz, 250 V_{p-p}) to a capacitively coupled[29] open cylindrical ICR cell for analysis. The robust automatic gain control[24] for transferring the same number of ions for each FT-ICR MS scan yielded less than 0.500 ppm rms mass error with external calibration. Each of the five most abundant ions were collisionally dissociated in the LTQ for low resolution MS/MS (3 microscans, 10,000 target ions, 2.0 Da isolation width, 35 % relative collision energy, 0.250 activation q, 30 ms activation period, and dynamic exclusion list size of 60 for 1 minute). Data was collected with Xcalibur 2.0 software (Thermo Fisher).

Following the *identification* of disulfide-containing peptides from the first pass low resolution LTQ MS/MS analysis (as described in Data analysis and Informatics section), the samples were re-analyzed by nano-LC, selected-ion high resolution MS/MS to confirm charge state and fragment ion assignments. The second experiment is needed for verification of disulfide connectivity. The scan type for the high resolution MS/MS was set at 7 to 10 scans per segment. The first scan was the same as the precursor ion scan found in the top-5 data-dependent experiment. The next 2 to 9 scans were set to select relevant ions (disulfide connected peptide fragments) for high resolution MS/MS. The 2 or 3 most abundant charge states (for relevant disulfide connected proteolytic fragment targets) were selected for high resolution MS/MS analysis because different charge states are known to fragment differently with CID.[30–32] A selected-ion high resolution MS/MS scan consisted of a target ion accumulation target of 50,000 ions with a 5 Da mass selection window, CID fragmentation in the LTQ (35.0 scaled collision energy, 0.250 activation q, and 30 ms activation period), and transfer to the cell for measurement. Low resolution MS/MS spectra exhibiting ambiguous fragment assignments were easily assigned by high resolution MS/MS based on charge state validation and mass

errors less than 0.500 ppm. High resolution MS/MS data were collected with both Xcalibur 2.0 and MIDAS software.

Electron capture dissociation (ECD) was performed with a custom-built 9.4 T FT-ICR and is known to specifically break disulfide bonds more readily than the polypeptide backbone.[33–35] Thus, disulfide bonds not verified by high resolution CID MS/MS were analyzed by ECD FT-ICR MS. Ions were selected with a quadrupole mass filter and accumulated in a second octopole for 1 second.[36] The ions were then transferred through multiple ion guides and trapped in an open-ended cylindrical Penning trap by gated trapping for ECD analysis.[37] Accurate mass and time-tag[38] knowledge of disulfide peptides from the top-5 data-dependent analysis of the different digest facilitated the use of "peak parking" with the Eksigent nano-LC. Namely, at the elution time for the peptide of interest, the flow rate was reduced from 400 nL/min to 50 nL/min so that 25 ECD spectra could be signal-averaged. Data acquisition was performed by use of a Predator data station and data analysis by MIDAS 3.4 software.[39]

Data Analysis and Informatics

Peaks from the Xcaliber files were extracted with a customized peak picking algorithm, thresholded at 10% of the maximum peak magnitude for low resolution MS/MS and 1% for high resolution MS. The resulting files were searched with MASCOT (Matrix Science, Cambridge, UK) against a custom-created database containing the wild-type and L126C mutant sequences. To aid in identification of the 4MT labeled cysteine, the mass of the 4-MT label (252.14739) was added to the MASCOT modification database. Results from MASCOT were visualized and validated with Scaffold (Proteomics Software, Portland, OR) software. After *identification* of the 4MT labeled peptide, the remaining disulfide peptides from each digest were *identified* by comparing high-resolution MS precursor ion measurements to values calculated from the elemental composition of the assigned peptides. High-resolution MS/MS and ECD fragment ion assignments were performed by hand.

RESULTS AND DISCUSSION

Intact Protein Analysis

FT-ICR MS can resolve protein isotopic distributions[40] and thus determine the charge state unambiguously based on the m/z separation between isotopic variants differing in elemental composition by $^{12}C_n$ vs. $^{13}C_1$ $^{12}C_{n-1}$.[41] Thus, before sequential proteolysis and LC MS analysis, the intact wild-type and L126C-4MT GM2AP were analyzed by direct infusion ESI FT-ICR MS (Figure 2). A 240 Da mass shift was observed between the two constructs, corresponding to the addition of one 4MT label to the substituted reporter cysteine (L126C). The spectra also show several salt and oxidation adducts, both common for intact protein analysis.

A second criterion for identification of the correct construct is presented in Figure 3, top. If there are less than four disulfide bonds, the 16+ charge state isotopic distribution, calculated from the molecular formula for the L126C-4MT GM2AP construct, will decrease by $0.12598 = (2)(1.007825)/16$ for each addition of 2 hydrogens. Thus, a positive match between the calculated and experimental isotopic distributions precedes downstream analysis. For this case, Figure 2, bottom illustrates excellent agreement between the measured and experimental isotopic distributions for the 16+ charge state isotopic distribution of the L126C-4MT GM2AP construct. Also, the salt adducts and oxidized species match the correct isotopic distribution (data not shown). Thus, mass analysis of intact L126C-4MT GM2AP unambiguously confirms the presence of four disulfide bonds and a single 4MT modification, but not disulfide bonding arrangement.

Tryptic Digest Peptide Analysis

Following tryptic digestion, the LC high-resolution precursor MS and low-resolution MS/MS data were searched with MASCOT against the known sequence of L126C GM2AP, allowing for the presence of 4MT. Low resolution MS/MS was chosen at first because of the slower duty cycle associated with high resolution MS/MS. Figure 4 (top) presents the sequence of L126C GM2AP, expected disulfide connectivity, location of the reporter cysteine, and sites of proteolytic cleavage for different proteases. MASCOT/Scaffold analysis identifies the tryptic digest fragments shown in blue in Figure 4, bottom), but cannot identify disulfide-containing peptides (red in Figure 4, bottom). MASCOT is typically used to analyze proteomic data sets in which the protein sample from cell lysate (including proteins containing disulfide bonds) has been reduced with dithiothreitol and alkylated with iodoacetamide. Thus, the peptides that contain cysteine will have reacted with iodoacetimide and can be identified with MASCOT. This experiment was designed to retain the disulfide connectivity. Our current version of MASCOT cannot identify peptides that are linked by disulfide bonds.

However, based on the known primary sequence, accurate mass measurement of the tryptic digest peptide precursor ions, and sequence tags from subsequent MS/MS, manual analysis revealed all of peptides containing *one or more* disulfide linkages, thus providing 100% sequence coverage. In addition, from Figure 4 (top), the connectivity for tryptic peptide Cys-1 (linking C^8 to C^{152}), containing a *single* disulfide bond (see Figure 5) could be uniquely determined (see below). Thus, from the predicted sequence and the results of the tryptic digest, the expected tryptic disulfide peptide sequences and masses could be generated. Because 100% sequence coverage *identification* was provided by trypsin digestion, other non-disulfide bound peptide fragments were not reported for the Trypsin/Glu C or Trypsin/Glu C/Asp N digestions. The need to *verify* the disulfide bound peptide fragments generated the need for the multiple digestion platform. Furthermore, high mass accuracy reduces the number of possible matches for a measured peptide to the possibilities found in a database (or protein) of known sequences. For example, if the tryptic peptide IESVLSSSGK, mass 1005.5342 Da, is searched against the possible peptide fragments from the sequence of GM2AP at 1, 20, and 2000 ppm mass error, the numbers of matched peptide sequences are 1, 4, and 7, respectively. Thus, high mass accuracy yields higher confidence in assignments by reducing the number of possible peptide matches.

Location of Spin-Labeled Cysteine

Figure 6 shows the observed b- and y-ion series for the tryptic peptide containing the 4MT reporter cysteine. In contrast to other labile post-translational modifications,[42–44] the present data illustrate that the 4MT thioester bond does not break during CID fragmentation, because the b_{9-15} and y_{13-14} ion series retain the mass associated with 4MT addition. Furthermore, if a population of the expressed protein were not properly folded, other non-reporter cysteine residues would be modified by the 4MT label. This is not the case because other 4MT modified non-reporter cysteine were not observed. Figure 6 thus establishes the sequence location of the 4MT spin-labeled cysteine.

Verification of Disulfide Bond Connectivity from Sequential Trypsin, Glu-C, and Asp-N Peptide Analysis

From the tryptic peptide assignments and the predicted subsequent Glu-C and AspN proteolytic cleavage sites, the remaining disulfide-connected peptides were generated and denoted as Cys-2a, Cys-2b, and Cys-2c (see Figure 5). Charge state m/z values are also calculated for nano-LC selected-ion high resolution MS/MS.

Figure 7 presents the fragment ions from the disulfide-containing peptides identified by high mass accuracy MS and CID MS/MS. From the trypsin digest, Cys-1 (Figure 7, top; Table 1)

resulted in b- and y- ions that retained the mass increase associated with the second, shorter LGCIK sequence. High resolution MS/MS provided unambiguous assignment of the fragment ions for Cys-1; i.e., at low resolution/mass accuracy in the LTQ (close to unit resolution) many of the fragments had assignment ambiguities (data not shown). From the trypsin/Glu C digestion, Cys-2a was verified (Figure 7, bottom; Table 2) with a tripeptide sequence tag.[45] The cysteine precursor ion mass measured to within 0.340 ppm mass error (Table 3) includes the loss of 2 hydrogens for the disulfide bond formed between C^{68} and C^{75}.

As for Cys-2 and Cys-2b, high resolution CID MS/MS provided a sequence tag for identification, but did not reveal the disulfide bond connectivity. Cys-2 and Cys-2b are essentially "cyclic" peptides, and are thus expected to fragment poorly by low-energy CID. [13, 14] Therefore, those peptides were fragmented by ECD. Both peptides resulted in only a charge-reduced species, not fragmentation (data not shown). The trypsin/Glu C sample was therefore digested with Asp N to release Cys-2c (Figure 5). Once again, high resolution MS/ MS sequencing could not verify the final two disulfide bonds; however, peptide identity was confirmed. Figure 8 presents the spectrum after "peak parking" nano-LC ECD FT-ICR MS. Once peak parking is initiated, i.e., flow rate slowed from 200 nL/min to 50 nL/min, the separation will be less than optimal for the remainder of the analysis. However, the ECD experiment was designed for analysis of only Cys-2c, thus the loss in separation efficiency for the remainder of the gradient was irrelevant. ECD is known to specifically fragment disulfide bonds.[33−35] In this case, ECD specifically broke the C^{94} – C^{105} disulfide bond to generate Frag2 (Figure 8) and $EPC^{94}PEPLR$. ECD analysis thus provided the final piece of evidence to verify the last two disulfide bonds.

Finally, Table 3 summarizes the tryptic peptides identified by MASCOT, along with the manually identified disulfide bonds. The data acquired from all three sequential digests by accurate mass measurement MS and MS/MS sequence tags resulted in quick identification of all four disulfide peptides as well as the sequence location of the 4MT-Cys.

CONCLUSIONS

A multi-tiered assay successfully *validates* protein folding for GM2AP mutants by use of conventional proteomic techniques and sequential digestion with a series of different proteases. Although sequential proteolysis digestion increased the compositional complexity of the sample (i.e., number of peptide fragments), the length of *individual* disulfide-containing peptides was *reduced*, thereby simplifying interpretation. The modified 14.5 T LTQ-FT ICR MS yielded mass errors of less than 1 ppm with automatic gain control (AGC). For external calibration coefficients to be applied on an LC time scale, the same number of ions must be transferred to the cell for each measurement.

High resolution MS combined with low-resolution MS/MS provides a quick screen for *identification* of the spin-labeled mutant peptide, protein sequence coverage, and disulfide bound peptide fragments. High resolution CID MS/MS allowed for *validation* of expected disulfide links. In cases for which high resolution CID MS/MS did not establish disulfide connectivity, ECD with the 9.4 T FT-ICR MS provided the necessary evidence. Finally, the present techniques can be easily applied to other GM2AP constructs produced for EPR studies, and more generally to other proteins with natural or artificial post-translational modifications and multiple disulfide linkages.

ACKNOWLEDGMENT

REFERENCES

1. Meier EM, Schwarzmann G, Furst W, Sandhoff K. J. Biol. Chem 1991;266:1879–1887. [PubMed: 1824846]

2. Mchaourab HS, Lietzow MA, Hideg H, Hubbell WL. Biochemistry 1996;35:7692–7704. [PubMed: 8672470]

3. Bertoni C, Li YT, Li SC. J. Biol. Chem 1999;274:28612–28618. [PubMed: 10497228]

4. Kolter T, Sandhoff K. J. Inherited Metabolic Disease 1998;21:548–563.

5. Huang JQ, Trasler JM, Igdoura S, Michaud J, Hanal N, Gravel RA. Human Molecular Genetics 1997;6:1879–1885. [PubMed: 9302266]

6. Wright CS, Li SC, Rastinejad F. J. Mol. Biol 2000;304:411–422. [PubMed: 11090283]

7. Columbus L, Hubbell WL. Biochemistry 2004;43:7273–7287. [PubMed: 15182173]

8. Bordignon E, Klare JP, Doebber M, Wegener AA, Martell S, Engelhard M, Steinhoff HJ. J. Biol. Chem 2005;280:38767–38775. [PubMed: 16157581]

9. Hubbell W, Cafiso D, Altenbach C. Nature Struct. Mol. Biol 2000;7:735–739.

10. Fanucci GE, Cafiso DS. Curr. Opin. Struct. Biol 2006;16:644–653. [PubMed: 16949813]

11. Mathias JD, Ran Y, Carter JD, Fanucci GE. Biophysical Journal 2009;77x

12. Lundblad, RL. Chemical Reagents for Protein Modification. Vol. 3 ed.. CRC Press; 2004.

13. Bean MF, Carr SA. Anal. Biochem 1992;201:216–226. [PubMed: 1632509]

14. Badock V, Raida M, Adermann K, Forssmann WG, Schrader M. Rapid Communications in Mass spectrometry 1998;12:1952–1956. [PubMed: 9842742]

15. Gorman JJ, Wallis TP, Pitt JJ. Mass Spectrom. Rev 2002;21:183–216. [PubMed: 12476442]

16. Xu H, Zhang L, Freitas MA. J. Proteome Res 2008;138–144:1.

17. Yen TY, Joshi RK, Yan H, Seto NOL, Palcic MM, Macher BA. J. Mass Spectrom 2000;35:990–1002. [PubMed: 10972999]

18. Yen TY, Yan H, Macher BA. J. Mass Spectrom 2002;31:15–30. [PubMed: 11813307]

19. Nair SS, Nilsson CL, Emmett MR, Schaub TM, Gowd KH, Thakur SS, Krishnan KS, Balaram P, Marshall AG. Anal. Chem 2006;78:8082–8088. [PubMed: 17134143]

20. Popolo L, Ragni E, Carotti C, Palomares O, Aardema R, Back JW, Dekker HL, de Koning LJ, de Jong L, de Koster CG. J. Biol. Chem 2008;283:18553–18565. [PubMed: 18468997]

21. Schaub TM, Hendrickson CL, Horning S, Quinn JP, Senko MW, Marshall AG. Anal. Chem 2008;80:3985–3990. [PubMed: 18465882]

22. Ran Y, Fanucci GE. Anal. Biochem 2008;382:132–134. [PubMed: 18694718]

23. Zhang S, Van Pelt CK, Henion JD. Electrophoresis 2003;24:3620–3632. [PubMed: 14613186]

24. Schwartz JC, Senko MW, Syka JEP. J. Am. Soc. Mass Spectrom 2002;13:659–669. [PubMed: 12056566]

25. Syka JEP, Marto JA, Bai DL, S H, Senko MW, Schwartz JC, Ueberheide B, Garcia B, Busby S, Muratore T, Shabanowitz J, Hunt DF. J. Proteome Red 2004;3:621–626.

26. Senko MW, Hendrickson CL, Pasa-Tolic L, Marto JA, White FM, Guan S, Marshall AG. Rapid Commun. Mass Spectrom 1996;10:1824–1828. [PubMed: 8953784]

27. Håkansson K, Chalmers MJ, Quinn JP, McFarland MA, Hendrickson CL, Marshall AG. Anal. Chem 2003;13:3256–3262.

28. Marshall AG, Guan S. Rapid Commun. Mass Spectrom 1996;10:1829–1832. [PubMed: 8953785]

29. Beu SC, Laude DA. Anal. Chem 1992;64:177–180.

30. Tang XJ, Thibault P, Boyd RK. Anal. Chem 1993;65:2824–2834. [PubMed: 7504416]

31. Griffiths WJ, Jonsson AP. Proteomics 2001;8:934–945. [PubMed: 11683510]

32. Tsapraili G, Nair H, Somogyi A, Wysocki VH, Zhong W, Futrell JH, Summerfield SG, Gaskell SJ. J. Am. Chem. Soc 1999;121:5142–5154.

33. Zubarev RA, Krunger NA, Fridriksson EK, Lewis M, AH DM, Carpenter BK. Journal of the American Chemical Society 1999;121:2857–2862.

34. Zubarev RA. Current Opinion in Biotechnol 2004;15:12–16.

35. Uggerud E. Int. J. Mass Spectrom 2004;234:45–50.

36. Senko MW, Hendrickson CL, Emmett MR, Shi SD, Marshall AG. J. Am. Soc. Mass Spectrom 1997;8:970–976.

37. Tsybin, Yl; Hendrickson, CL.; Beu, SC.; Marshall, AG. Int. J. Mass Spectrom 2006:144–149.

38. Pasa-Tolic L, Masselon CD, Barry RC, Shen Y, Smith RD. BioTechniques 2004;37:621–636. [PubMed: 15517975]

39. Blakney, GT.; Robinson, DE.; Ly, NV.; Kelleher, NL.; Hendrickson, CL.; Marshall, AG. 53rd Amer. Soc. Mass Spectrom. Ann. Conf. on Mass Spectrom. & Allied Topics; June 4–9, 2005; San Antonio, TX.

40. Hendrickson CL, Emmett MR. Ann. Rev. Phys. Chem 1990;50:517–513. [PubMed: 10575730]

41. Senko MW, Beu SC, McLafferty FW. J. Am. Soc. Mass Spectrom 1995;6:52–56.

42. Cooper HJ, Håkansson K, Marshall AG. Mass Spectrom. Rev 2005;24:201–222. [PubMed: 15389856]

43. Syka JEP, Coon JJ, Schroeder MJ, Shabanowitz J, Hunt DF. 2004;101:9528–9533.

44. Beausoleil SA, Jedrychowski M, Schwartz D, Elias JE, Villén J, Li J, Cohn MA, Cantley LC, Gygi SP. Proc. Natl. Acad. Sci., U.S.A 2004;101:12130–12135. [PubMed: 15302935]

45. Mørtz E, O'Connor PB, Roepstorff P, Kelleher NL, Wood TD, McLafferty FW, Mann M. Proc. Natl. Acad. Sci. U.S.A 1996;93:8264–8267. [PubMed: 8710858]

4-Maleimide-TEMPO

$$C_{13} \, H_{19} \, O_3 \, N_2$$
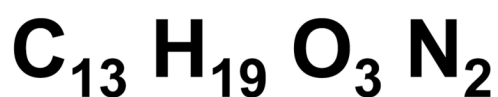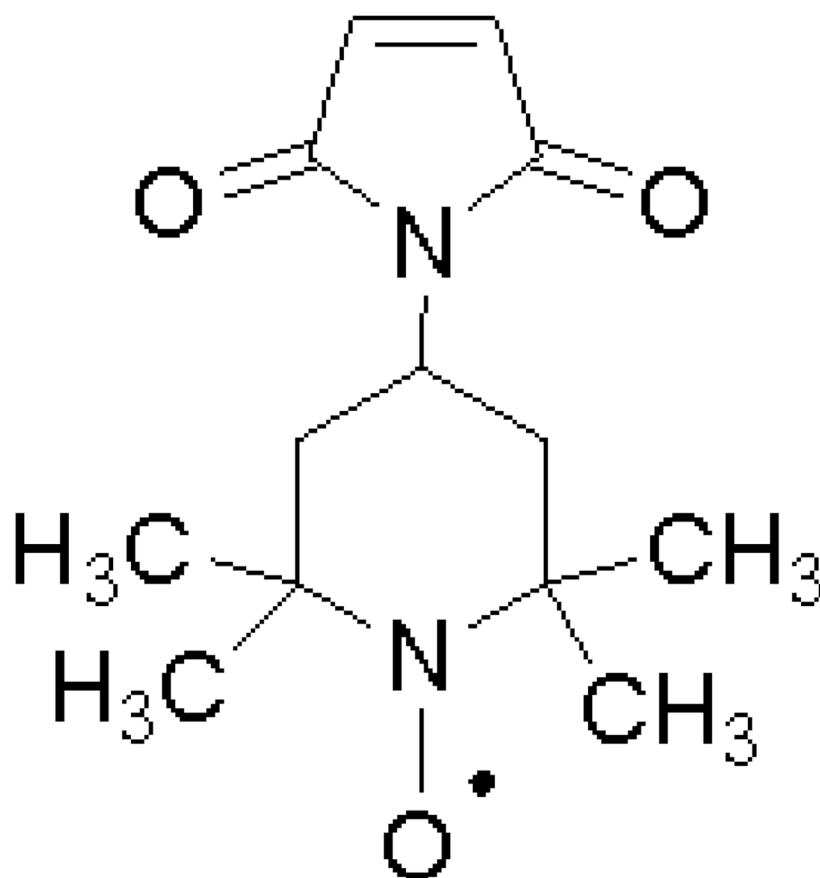
Molecular Weight = 251.14011 Da

Figure 1.
Structure, molecular weight, and elemental composition for 4-maleimide-TEMPO.
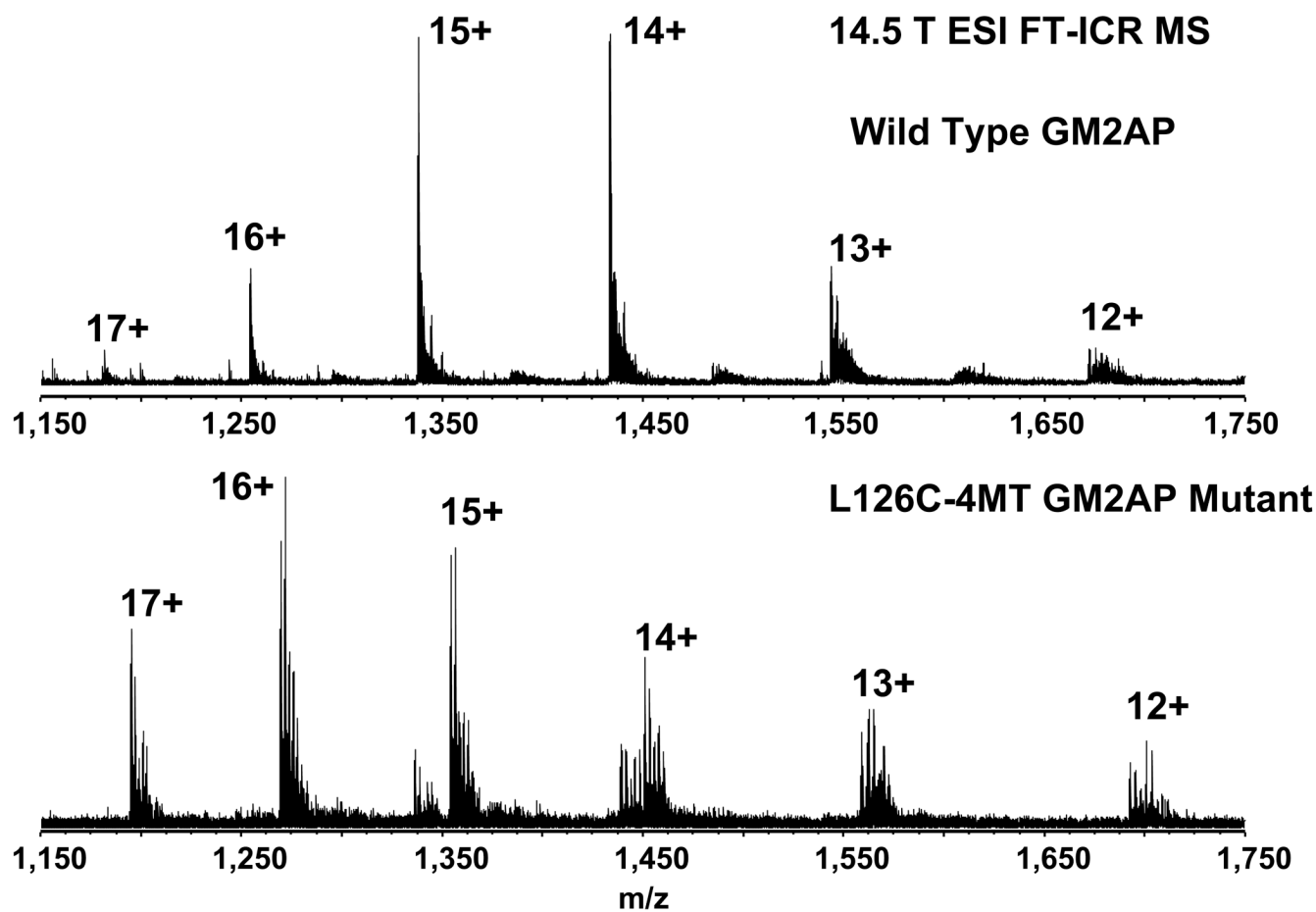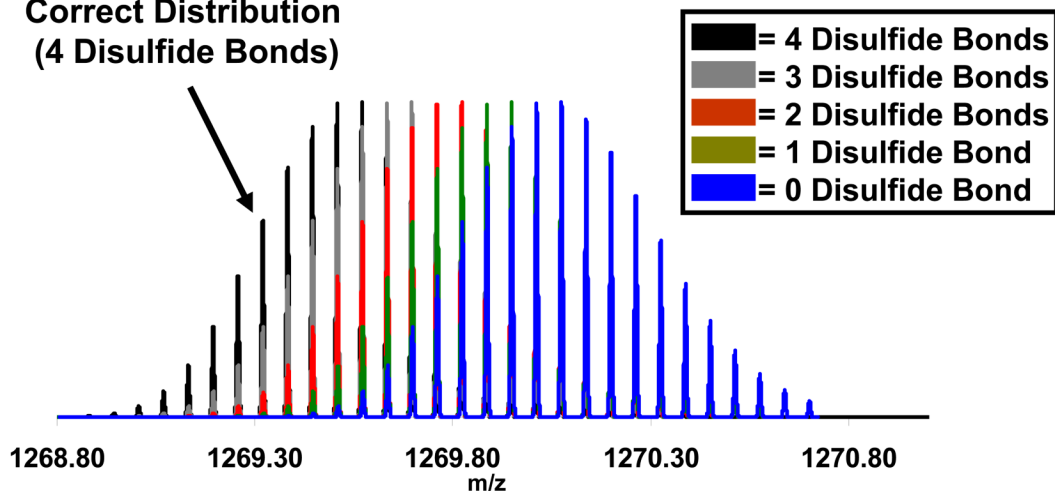
Figure 2.
Broadband 14.5 T electrospray positive-ion FT-ICR mass spectra of intact wild-type and L126C-4MT mutant GM2AP proteins. The L126C mutant was labeled with 4-maleimide-TEMPO. The shift in the m/z for the observed charge states indicates labeling of the protein.

Calculated Isotopic Distributions for L126C GM2AP (16+ Charge State)

Correct Distribution (4 Disulfide Bonds)

■	= 4 Disulfide Bonds
▨	= 3 Disulfide Bonds
■	= 2 Disulfide Bonds
■	= 1 Disulfide Bond
■	= 0 Disulfide Bond

1268.80   1269.30   1269.80   1270.30   1270.80

m/z

Isotopic Distribution for L126C-4MT GM2AP with 4 Disulfide Bonds

Exptl m/z	Calc'd m/z	ppm error
1269.4461	1269.4455	-0.465
1269.5088	1269.5082	-0.481
1269.5713	1269.5708	-0.378
1269.6340	1269.6335	-0.417
1269.6968	1269.6961	-0.575
1269.7594	1269.7587	-0.543

$[M+16H]^{16+}$

■ **Experimental**

■ **Calculated**

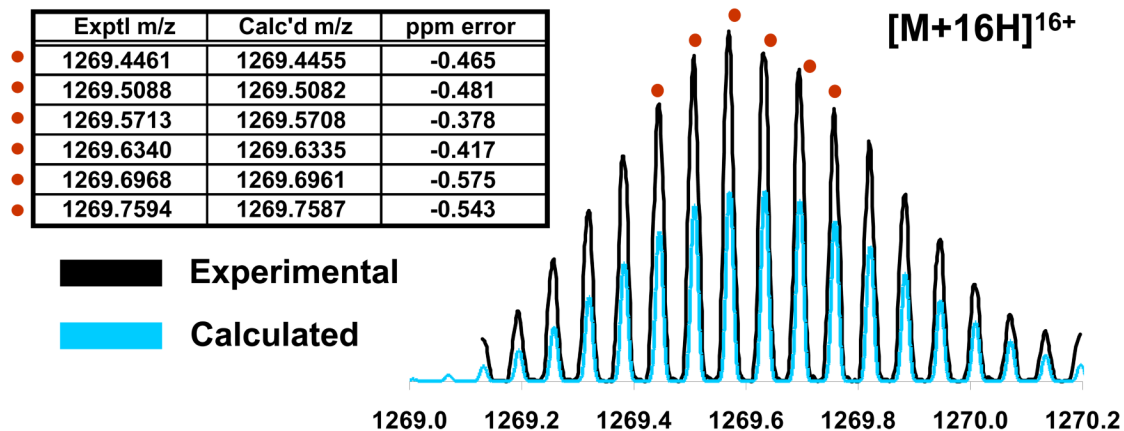1269.0 1269.2 1269.4 1269.6 1269.8 1270.0 1270.2

Figure 3.
Top: Calculated isotopic distributions corresponding to 0, 1, 2, 3, and 4 disulfide bonds for L126C-4MT GM2AP $[M+16H]^{16+}$. The calculated m/z distribution decreases by (2) (1.007825)/16 = 0.1260 for each additional disulfide linkage. Bottom: Calculated and experimental isotopic distributions for L126C-4MT GM2AP $[M+16H]^{16+}$. The close fit of the calculated to the experimental distribution confirms that the protein has the correct amino acid sequence, with four disulfide bonds, and a single 4MT label on a cysteine residue. The five highest-magnitude in the isotopic distribution were chosen for comparison to calculated masses (red dots).

L126C GM2AP

GHHHHHHHHHHSSGHIEGRHMSSFSWD**N**C**[8]**D**E**GK**D**P

AVI**R**SLTLE**P**D**PIVVPGNVTLSVVGSTSVPLSSPL**K**V**D**LV

LE**K**E**VAGLWI**K**IP**C**[68]**T**D**YIGS**C**[75]**TFE**HF**C**[81]**D**VL**D**MLIPT

GEP**C**[94]**PEPL**R**TYGLP**C**[105]**H**C**[107]**PF**K**E**GTYSLP**K**SEFVVP

D**C**[126]**ELPSWLTTGNY**RIE**SVLSSSG**KR**LG**C**[152]**IKIAASL**K**G

K, R: Trypsin
E: Glu-C
D: Asp-N

L126C-4MT GM2AP Sequence Coverage after Solution Trypsin Digestion and LC/MS

GHHHHHHHHHHSSGHIEGRHMSSFSWDMCDEGK**DP**
AVIRSLTLEPDPIVVPGNVTLSVVGSTSVPLSSPLKVDL
VLEKEVAGLWIKIPCTDYIGSCTFEHFCDVLDMLIPTGE
PCPEPLRTYGLPCHCPFK**EGTYSLPKSEFVVPD**C**[126]**
ELPSWLTTGNYRIESVLSSSGKRLGCIKIAASLKGI

———— **MASCOT Identification**
———— **Manual Identification**

Figure 4.
Top: L126C GM2AP amino acid sequence with location of reported disulfide bonds and predicted cleavages for trypsin (blue: K,R), Glu C (dark green: E), and Asp N (orange: D). The location of the L126C amino acid substitution is shown in bright green. The HIS_{10}-tag (light gray) is engineered to include a Factor Xa cleavage site. Bottom: Sequence coverage for the L126C-4MT GM2AP construct after trypsin digestion and nano-LC MS analysis. The blue sequence was identified by MASCOT; the red sequence was identified by hand, and corresponds to the peptides still containing disulfide bonds.

Expected Disulfide Peptides: Calculated Mass and m/z

Tryptic Disulfide Peptides

HMSSFSWDN**C**[8]DEGKDPAVIR

LG**C**[152]I K

Cys1: M_r = 2823.2777 Da
3+ = 942.09986
4+ = 706.82671
5+ = 565.66282

IP**C**[68]TDYIGS**C**[75]TFEHF**C**[81]DVLDMLIPTGEP**C**[94]PEPLR

Cys2: Mr = 5069.2368 Da
6+ = 845.88007
7+ = 725.18396
8+ = 634.66187

TYGLP**C**[105]H**C**[107]PFK
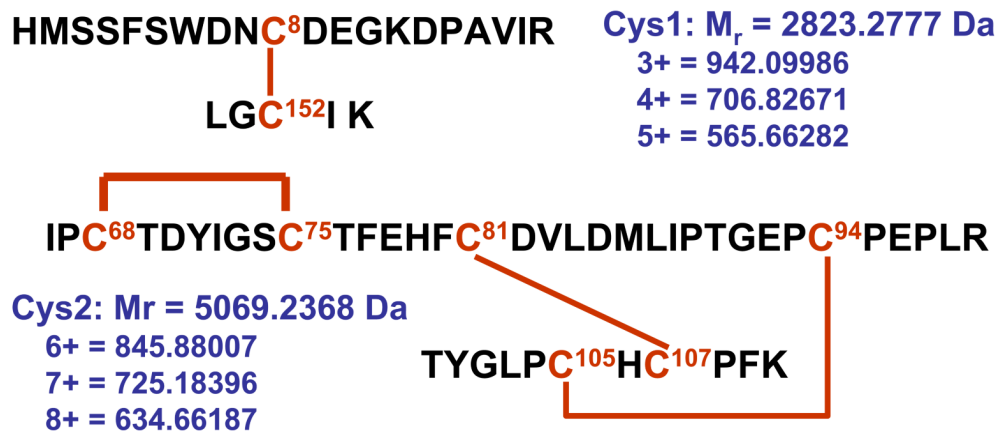
Tryptic/Glu C Disulfide Peptides

IP**C**[68]TDYIGS**C**[75]TFE

Cys2a: Mr = 2563.2172 Da
3+ = 855.07727
4+ = 641.55977

Cys2b: Mr = 3641.6635 Da
4+ = 911.42314
5+ = 729.33997
6+ = 607.95119

HF**C**[81]DVLDMLIPTGEP**C**[94]PEPLR

TYGLP**C**[105]H**C**[107]PFK
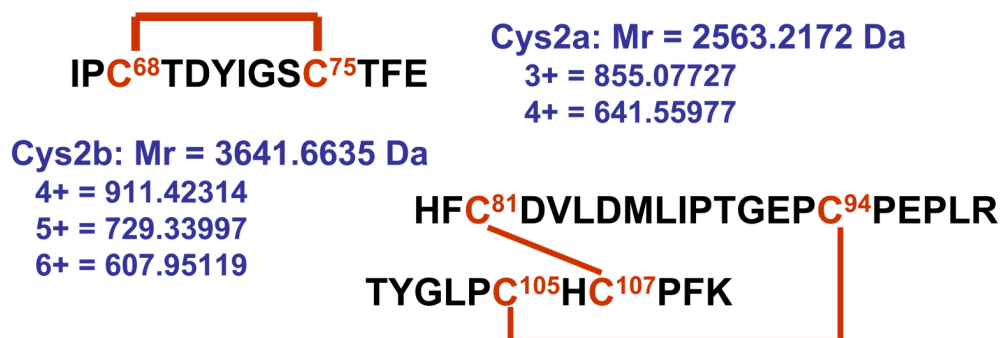
Tryptic/Glu C/Asp N Disulfide Peptide

Cys2c: Mr =2605.1374 Da
3+ = 869.38640
4+ = 652.29162
5+ = 522.03475

HF**C**[81]   EP**C**[94]PEPLR

TYGLP**C**[105]H**C**[107]PFK

Figure 5.
Scheme presenting the theoretical disulfide bound peptides after sequential proteolytic digestion. Various m/z values were calculated for charge states to aid during analysis and the selected ion monitoring MS/MS experiment. Other combinations were also calculated (not shown) but not identified.
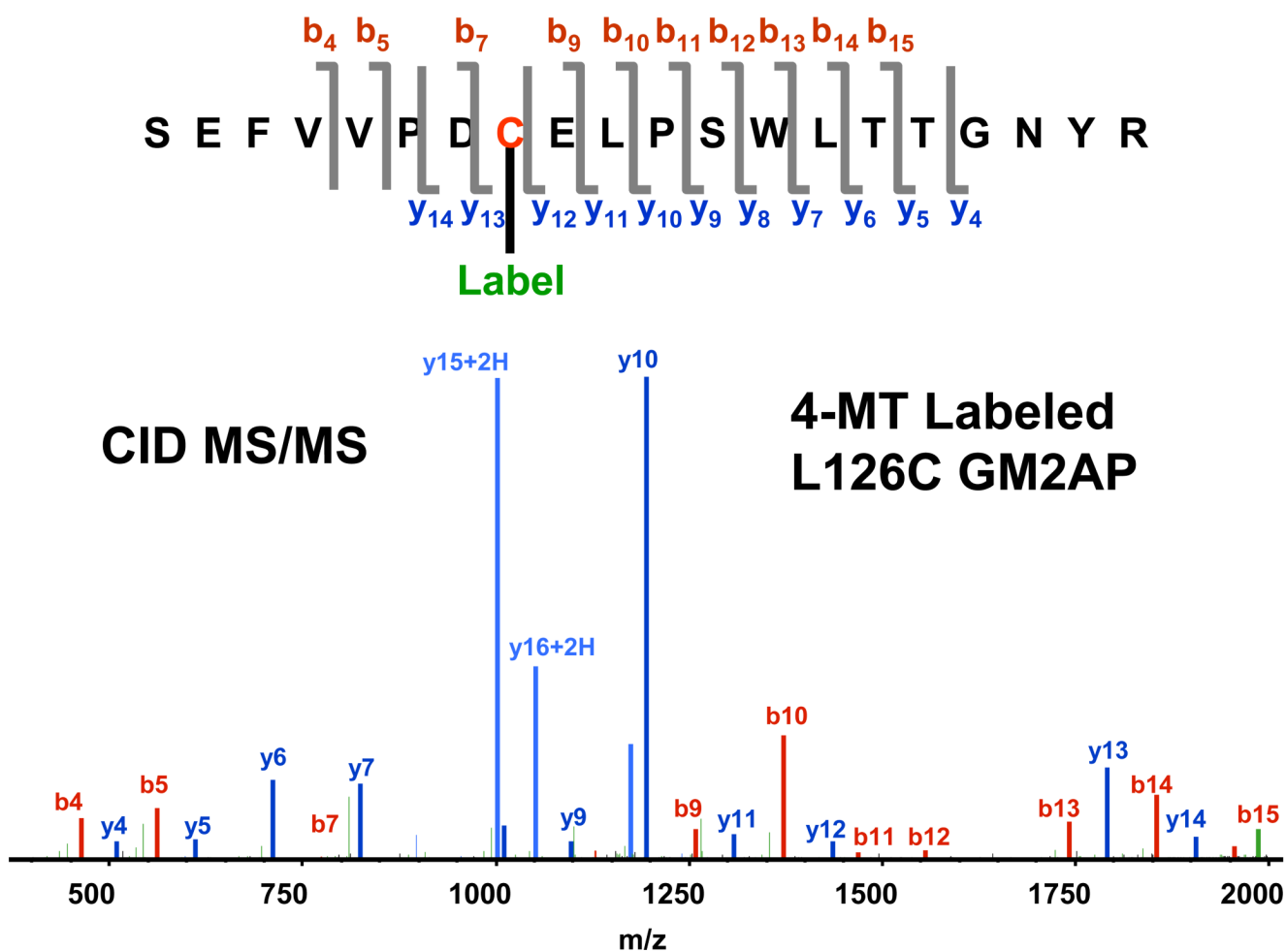
Figure 6.
Identified fragments for low-resolution CID MS/MS of tryptic digested 4MT L126C reporter cysteine. The same 4MT labeled reporter cysteine was also observed from the other digests (data not shown).
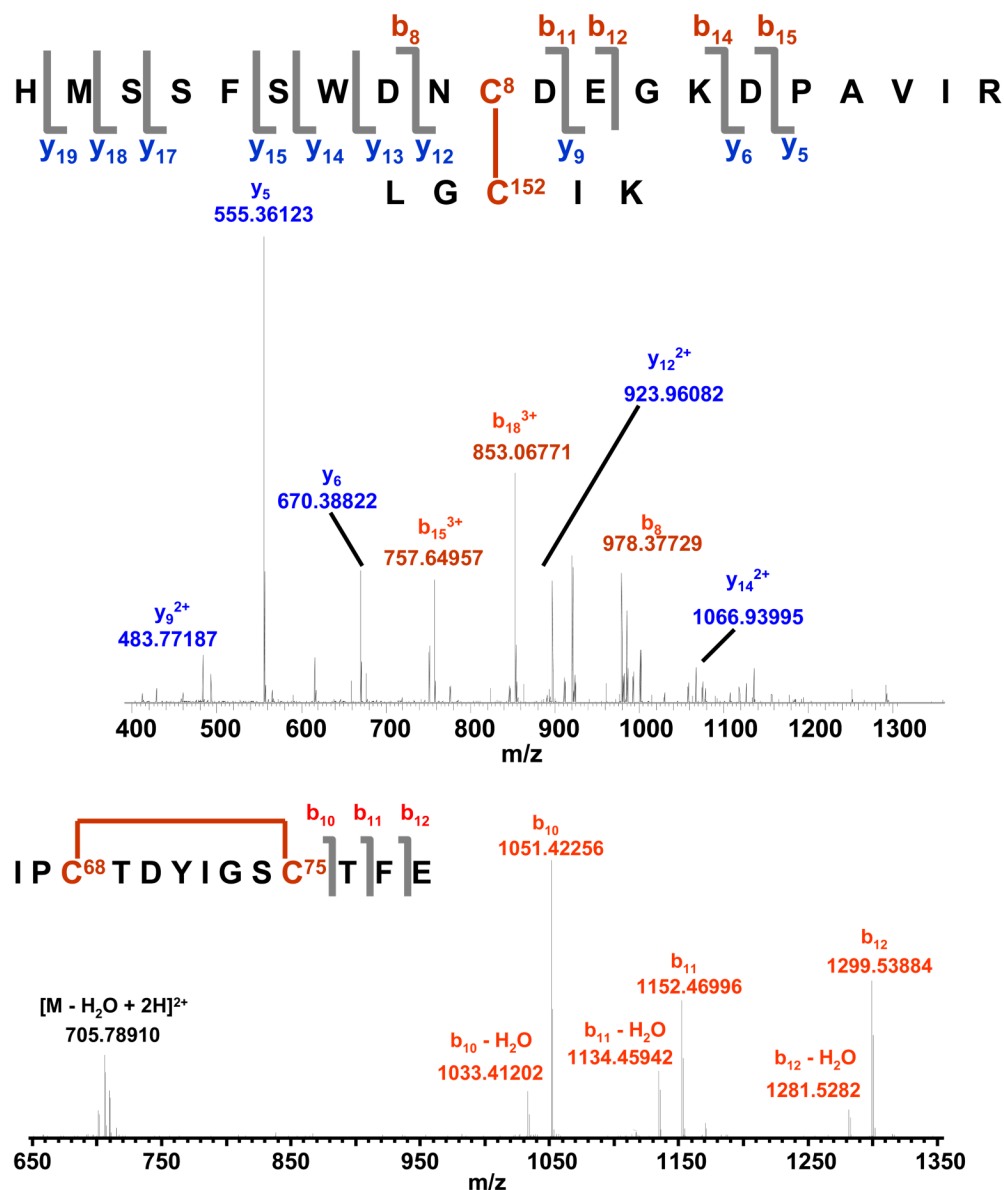
Figure 7.
Disulfide bonds that were verified through CID MS/MS analysis. Top: High-resolution MS/MS of Cys-1. Several large peptide fragment masses verify the peptide sequence. Bottom: High-resolution MS/MS of Cys-2a (mass scale-expanded segment shown as an inset). The calculated mass for the intact peptide matches the experimental mass corresponding to one disulfide bond (Table 1). A sequence tag of three amino acids verifies the identity of the disulfide-containing peptide. As expected, the cyclic disulfide bond peptide does not yield fragments.

Ion	Exptl m/z	Calc'd m/z	Error (ppm)
Frag2	1667.7072	1667.7046	1.6
Frag2 - H_2O	1649.7037	1649.6941	4.8
Frag2 - H_2O - NH_4	1632.6663	1632.667	-0.4
EPCPEPLR	939.4465	939.4478	-1.4
EPCPEPLR – H_2O	922.4451	922.4465	-1.5

Frag2 =

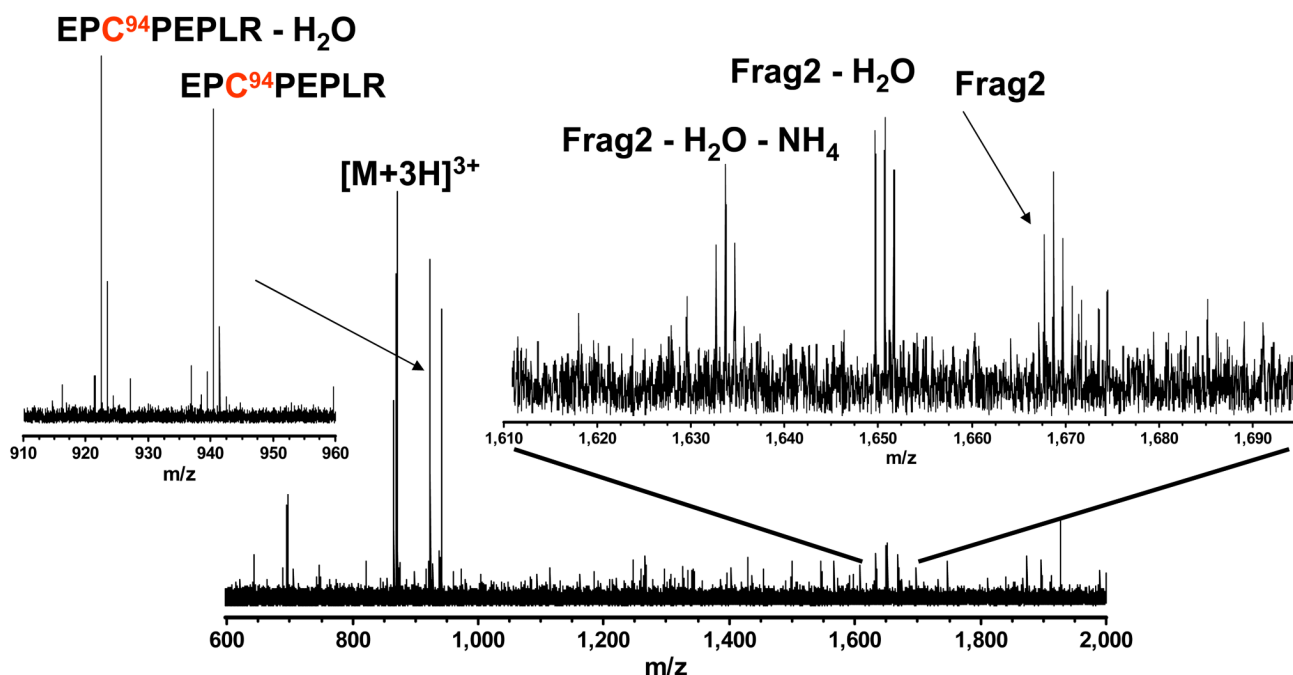HFC^{81}

$TYGLPC^{105}HC^{107}PFK$

Figure 8.
"Peak-parked nano-LC" high-resolution ECD MS/MS (25 scans, 3 min). ECD typically breaks disulfide bonds prior to amino acid backbone fragmentation. Two fragments corresponding to the specific fragmentation of the C^{94}-C^{105} disulfide bond were observed. The table lists the mass accuracy for ECD analysis.

Table 1

Peak list and mass errors from high-resolution CID MS/MS of Cys-1.

Ion	Charge	Exptl m/z	Exptl Mass (Da)	Calc'd Mass (Da)	Error (ppm)
b$_8$	1	978.3773	977.3700	977.3696	0.466
b$_{11}$	2	920.8761	1839.7377	1839.7383	−0.348
b$_{11}$-H$_2$O	2	911.8707	1821.7269	1821.7277	−0.478
b$_{12}$	2	985.3975	1968.7805	1968.7809	−0.223
b$_{14}$	2	1077.9551	2153.8957	2153.8973	−0.761
b$_{15}$	2	1135.4694	2268.9243	2268.9242	0.026
b$_{15}$	3	757.3150	2268.9232	2268.9242	−0.447
b$_{15}$-H$_2$O	3	751.3115	2250.9127	2250.9136	−0.420
y$_5$	1	555.3612	554.3539	554.3535	0.821
y$_9$	2	492.7772	983.5399	983.5395	0.386
y$_9$-H$_2$O	2	483.7719	965.5293	965.5295	−0.212
y$_{12}$	2	923.9610	1845.9075	1845.9081	−0.347
y$_{12}$	3	616.3098	1845.9076	1845.9081	−0.279
y$_{13}$	2	981.4744	1960.9343	1960.9351	−0.428
y$_{14}$	2	1074.5148	2147.0151	2147.0144	0.307
y$_{15}$	2	1118.0305	2234.0465	2234.0464	0.027
y$_{17}$	2	1235.0806	2468.1467	2468.1469	−0.097
y$_{18}$	3	852.7333	2555.1781	2555.1789	−0.319
y$_{19}$	3	896.4133	2686.2181	2686.2194	−0.490

Table 2

Peak list and mass errors from high-resolution CID MS/MS of Cys–2a.

Ion	Charge	Exptl m/z	Exptl Mass (Da)	Calc'd Mass (Da)	Error (ppm)
M-2H$_2$O	2	705.7891	1409.5637	1409.5631	0.390
b$_{10}$	1	1051.4226	1050.4153	1050.4150	0.271
b$_{10}$-H$_2$O	1	1033.4120	1032.4047	1032.4044	0.286
b$_{11}$	1	1152.4700	1151.4627	1151.4627	0.004
b$_{11}$-H$_2$O	1	1134.4594	1133.4521	1133.4521	0.013
b$_{12}$	1	1299.5388	1298.5316	1298.5311	0.358
b$_{12}$-H$_2$O	1	1281.5282	1280.5209	1280.5205	0.308

Table 3

Peak list and mass error for relevant peptides. The * indicates the spin-labeled L126C mutant peptide. Figure 4 lists the sequences for the different cysteine-containing peptides.

Exptl m/z	Exptl Mass (Da)	Calc'd Mass (Da)	Error (ppm)	Peptide
568.2611	2269.0151	2269.0148	0.138	GHHHHHHHHHHHHSSGHIEGR
670.3882	669.3810	669.3810	0.021	DPAVIR
1601.8937	3201.7728	3201.7747	−0.596	SLTLEPDPIVVPGNVTLSVVGSTSVPLSSPLK
408.2472	814.4799	814.4800	−0.110	VDLVLEK
458.2685	914.5224	914.5225	−0.084	EVAGLWIK
447.7318	893.4490	893.4494	−0.456	EGTYSLPK
855.7492	2564.2256	2564.2257	−0.014	SEFVVPDc*ELPSWLTTGNYR
503.7744	1005.5342	1005.5342	0.015	IESVLSSSGK
706.8267	2823.2777	2823.2777	0.000	Cys-1
845.8801	5069.2368	5069.2374	−0.120	Cys-2
723.7993	2562.2109	2562.2100	0.340	Cys-2a
911.4231	3641.6632	3641.6636	−0.126	Cys-2b
869.3866	2605.1378	2605.1378	−0.002	Cys-2c